Lawrence Berkeley National Laboratory

Title

Airfoil sampling of a pulsed Laval beam with tunable vacuum ultraviolet (VUV) synchrotron ionization quadrupole mass spectrometry: Application to low--temperature kinetics and product
detection

Permalink

Author

Soorkia, Satchin

Publication Date

2012-01-27

Airfoil sampling of a pulsed Laval beam with tunable vacuum ultraviolet (VUV) synchrotron ionization quadrupole mass spectrometry: Application to low-temperature kinetics and product detection

Satchin Soorkia[1,#], Chen-Lin Liu[1,2,†], John D. Savee[3], Sarah J. Ferrell[2], Stephen R. Leone[1,2] and Kevin R. Wilson[2,*]

[1]Departments of Chemistry and Physics, University of California, Berkeley, CA 94720, USA

[2]Chemical Sciences Division, Lawrence Berkeley National Laboratory, 1 Cyclotron Road, Berkeley, CA 94720, USA

[3]Combustion Research Facility, Mail Stop 9055, Sandia National Laboratories, Livermore, CA 94551, USA

[#] Current address:

Institut des Sciences Moléculaires d'Orsay

Université Paris-Sud 11, CNRS UMR 8214

91405 Orsay, FRANCE

[†] Current address:

National Synchrotron Radiation Research Center (NSRRC)

Hsinchu 30076, Taiwan

[*] Correspondence to: krwilson@lbl.gov

Abstract

A new pulsed Laval nozzle apparatus with vacuum ultraviolet (VUV) synchrotron photoionization quadrupole mass spectrometry is constructed to study low-temperature radical-neutral chemical reactions of importance for modeling the atmosphere of Titan and the outer planets. A design for the sampling geometry of a pulsed Laval nozzle expansion has been developed that operates successfully for the determination of rate coefficients by time-resolved mass spectrometry. The new concept employs airfoil sampling of the collimated expansion with excellent sampling throughput. Time-resolved profiles of the high Mach number gas flow obtained by photoionization signals show that perturbation of the collimated expansion by the airfoil is negligible. The reaction of C_2H with C_2H_2 is studied at 70 K as a proof-of-principle result for both low-temperature rate coefficient measurements and product identification based on the photoionization spectrum of the reaction product versus VUV photon energy. This approach can be used to provide new insights into reaction mechanisms occurring at kinetic rates close to the collision-determined limit.

1. Introduction

Invented by Gustaf de Laval in 1888 for use in steam turbines, Laval nozzles have proven to be the ideal tool to generate uniform supersonic expansions for the study of low-temperature radical-neutral chemical reactions. These convergent-divergent shaped nozzles produce collimated flows at a constant Mach number. As a consequence, the temperature and density at all points within the flow is constant in theory and, in practice, nearly so.[1] Thermally equilibrated gaseous environments ($10 < T < 300$ K and $0.1 < P < 10$ Torr) are generated for axial distances exceeding a few tens of centimeters with no temperature or density gradients. Because local equilibrium is maintained at all points, the post-nozzle flow is often referred to as a "wall-less flow tube reactor" in which reactions involving reagents with very low vapor pressures, that otherwise would tend to condense, can be studied.[2] Laval nozzles have found a unique application as a method for producing gas flows suitable for kinetic studies of chemical reactions in low-temperature environments such as those encountered in planetary atmospheres.

The Cassini-Huygens mission has provided a substantial increase to our knowledge of Titan's atmosphere. In particular, the complexity of the photochemical processes that drive its atmospheric composition has proven to be far beyond our expectations.[3,4] Over the last few decades, detailed models[5] have been developed to account for space-based observations. However, to date less than 10% of the rates concerning neutral species have been measured in the relevant temperature range.[6] As a consequence, the accuracy of these photochemical models[6] is greatly affected and it has been suggested that discrepancies between modeling and observations may arise from the lack of concrete kinetic data.[7] The extrapolation of room temperature measurements to low temperatures via Arrhenius-type laws is commonly used as a source of kinetic data in these models, but is known to be problematic for radical-neutral chemical reactions.[8] Often, the rate coefficient is found to exhibit a negative temperature dependence, which is an indication of a complex kinetic behavior. The rate of chemical reactions and their dependence as a function of temperature is of central importance to validate and improve the predictive capability of the proposed photochemical models for Titan. To surmount this obstacle and limit kinetic uncertainties, both rate constants and product branching

fractions for the reactions included in photochemical models need to be experimentally determined.

During the past three decades, significant progress has been made in using Laval nozzles to study chemical kinetics of key reactions down to the low temperatures relevant to Titan's atmosphere. Rowe and coworkers[9,10] pioneered the CRESU technique (Cinétique de Réaction Chimique en Ecoulement Supersonique), which uses a continuous Laval expansion to study chemistry under planetary atmospheres conditions. Smith and coworkers designed and characterized uniform pulsed supersonic expansions, resulting in gas flows with comparable beam characteristics to a continuous flow but requiring much smaller pumping capacities and reagent quantities.[11,12] The flexibility of the pulsed technique has led to its adoption by Leone and coworkers,[13] Abel and coworkers[2] and Heard and coworkers.[14]

To date, low-temperature chemical kinetics of radical-neutral reactions are studied using either a chemiluminescence tracer method or laser induced fluorescence (LIF) to detect the time evolution of transient species such as CH,[15] C_2H,[16,17] C_4H[18] or CN[19] radicals. However, photon-based techniques are limited to species that have accessible spectroscopic transitions. Mass spectrometry is, in principle, a more universal detection technique that simplifies the measurement of kinetics and detection of multiple species. Furthermore, mass spectrometry coupled to tunable vacuum ultraviolet (VUV) synchrotron photoionization, unlike optical-based techniques, can be used to identify reaction products as well as radical intermediates, thus greatly enhancing the information content in a single measurement. For example, tunable VUV photoionization mass spectrometry can be used to determine the isomeric composition of various reaction products, thus affording new insights into detailed reaction mechanisms, as demonstrated by the multiplexed photoionization mass spectrometer constructed by Osborn and coworkers.[20-22]

However, there are significant experimental challenges that need to be addressed when sampling a pulsed Laval beam for mass spectrometric analysis. Lee and coworkers[13] developed skimmer sampling of a pulsed Laval expansion. The feasibility of

this approach using 118 nm laser radiation for ionization and time-of-flight mass spectrometry (TOF-MS) to make direct measurements of rate coefficients by monitoring reaction products was demonstrated in that early work. Very recently, Sabbah and coworkers[23] successfully extended this approach to experimental measurements on the kinetics of pyrene dimerization.

In this paper, we describe a pulsed Laval nozzle apparatus employing tunable VUV synchrotron photoionization for the study of radical-neutral chemical reactions. With this instrument, transient species and reaction products are monitored both in time and as a function of VUV synchrotron photon energy. A detailed description of the apparatus is provided, which combines tunable VUV synchrotron light at the Chemical Dynamics Beamline of the Advanced Light Source with mass spectrometry[20] to probe: (1) low-temperature kinetics and (2) isomeric product branching ratios of radical-neutral chemical reactions (to be reported in a future paper). We have reconsidered both the sampling geometry of the pulsed Laval expansion and its impact on the validity of kinetic measurements using mass spectrometry techniques.[24] Details are presented for how this important sampling geometry aspect of the new instrument is addressed by the design of a novel symmetric airfoil-shaped sampling arrangement.

2. Laval apparatus with quadrupole mass spectrometry

A supersonic pulsed Laval nozzle expansion apparatus with synchrotron VUV ionization and quadrupole mass spectrometry is constructed for the study of kinetics and isomeric product branching of gas phase radical-neutral chemical reactions at low temperatures. It consists of two pulsed valves injecting trace amounts of the radical precursor and reactant seeded in the main N_2 through a Laval nozzle to produce a thermally equilibrated low-temperature expansion. After uniform conditions are achieved in the molecular beam, the radical-neutral chemical reaction is initiated by pulsed laser photolysis of the radical precursor, which creates a uniform density of radicals along the axis of the flow. Transient species and reaction products are probed using tunable VUV photoionization quadrupole mass spectrometry. As can be seen in the section view shown in Figure 1, a symmetric airfoil-shaped device separates the source chamber (0.1 − 1 Torr) from the detection chamber (low 10^{-7} Torr) and is used to sample the Laval beam

with limited perturbations to the collimated expansion through a 450 μm pinhole. The reactive gases are then photoionized within 1 mm after the pinhole by the tunable VUV synchrotron radiation at the Advanced Light Source and the resulting ions are detected continuously via a quadrupole mass spectrometer.

This section is divided into four parts: (a) the Laval nozzle expansion chemical reactor and vacuum system, (b) the airfoil sampling of the collimated expansion, (c) validity of kinetics measurements and (d) the detection chamber and quadrupole mass spectrometer (QMS) which are described in detail below.

2.1. Laval nozzle expansion chemical reactor and vacuum system

Figure 1 shows a sectional view of the pulsed Laval apparatus. The Laval nozzle block is based upon the original design described by Lee and coworkers.[13] Briefly, the block consists of two pulsed valves (Parker General valves) supplying gas to a Laval nozzle, which produces a thermally equilibrated collimated low-temperature gas flow. The stagnation pressure in the pre-expansion reservoir is monitored using a pressure transducer (Omega PX170 series). A quartz window is mounted on the block to transmit the excimer laser for coaxial laser photolysis along the collimated Laval expansion. The nozzle assembly is mounted on a linear translator (200 mm travel) driven from outside the chamber. The Mach number 4 nozzle used in this study has been previously characterized.[13]

The main carrier gas, N_2, as well as the radical precursor is supplied from gas cylinders through stainless steel lines to the pulsed valves. The flows are monitored by individually calibrated mass flow controllers (MKS Mass-Flo Analog). Condensable gases such as 1,3-butadiene are kept in a cold bath at (278 K) to lower their vapor pressure, thus preventing condensation in the gas lines. The purities of the gases used in the experiments reported here are as follows: N_2 (99.999%), acetylene (99.6%), and 1,3-butadiene (99% Sigma Aldrich). The acetylene tank is equipped with an activated charcoal cartridge filter located prior to the mass flow controller to remove acetone, which is present in the tank as a stabilizing agent. The gases are injected into a stainless

steel cell (150 cm^3 in volume) to achieve homogeneous mixing prior to flowing into the pre-expansion region of the pulsed Laval nozzle as described previously.[13]

The pressure in the source chamber is measured with an absolute capacitance manometer (MKS Type 722B). A Roots pump (Edwards QMB 1200) backed by a dry pump (Edwards IDP 80), providing a typical pumping speed of 950 m^3/h at 0.15 Torr, evacuates the majority of gases composed of the carrier gas (N$_2$), the radical precursor in trace amounts, and slip gas. With this combination of pumps and slip gas, the pressure inside the source chamber can be adjusted to better than 1 mTorr in the 0.1 − 1 Torr range. Uniform flow conditions along the axis of the Laval expansion can be achieved by using a slip gas (N$_2$), which is introduced by a manual leak valve into the source chamber. Ideally, the optimal collimation of the Laval beam is reached when the background pressure is equal to the static flow pressure. By monitoring the impact pressure with a pressure transducer along and perpendicular to the axis of the flow over a distance of ~20 cm and adjusting the slip gas flow rate, uniform expansion conditions can be obtained.

Radical species (e.g. C$_2$H, C$_3$H$_3$, CH$_3$) are generated coaxially within the uniform expansion by pulsed laser photolysis of the precursor using an unfocused excimer beam at 193 nm (Lambda Physik COMPex Pro 110). The throat of the Laval nozzle limits the diameter of the laser beam to 1 cm in diameter. Radical precursors are photolysed with ~10 mJ/cm^2 laser pulses (typical pulsewidth of 20 ns at 193 nm) measured after the divergent section of the nozzle. Concentrations of these species in the flow are monitored by VUV photoionization mass spectrometry as described later in this section.

2.2. Airfoil sampling of collimated expansion

Sampling methods in molecular beams mass spectrometry can perturb the ideal conditions of the initial gas flow and therefore requires a careful design. Lee and coworkers[13] implemented a skimmer sampling geometry into a pulsed Laval expansion. The critical features in their validation of this method were found to be the shape of the skimmer and the distance from the skimmer to flat walls orthogonal to the direction of the gas flow in the vacuum chamber. Shown in Figure 2 is a comparison between the

sampling configuration using (a) the airfoil developed here and (b) a 6 cm long 30° entrance cone skimmer by Lee and coworkers. In that earlier work, the effective pumping speed of the residual gases that are thermalized in front of the skimmer by hitting the chamber walls was also found to be of critical importance. Indeed, with a small cone-shaped skimmer (2 cm long, 1.5 cm diameter base on a 3 cm extension from the flat end wall) no distinctive gas pulse concentration profile could be observed with 118 nm laser photoionization and TOF-MS detection. It was proposed that residual thermalized gases originating from the chamber walls adjacent to the skimmer (see Figure 2(b)) were reflected back into the Laval expansion, which introduced perturbations to the collimated gas flow. To address this, a 3 cm extension tube was added to move the skimmer further from the end wall. This arrangement produced a highly perturbed gas pulse with a long "tail" (> 20 ms) for a nominal 5 ms gas pulse. Because of the highly perturbed concentration profile, it was difficult to make a precise determination of the arrival times of the gases in the detection region. In a further modification in that earlier work, a 30° entrance angle and 6 cm long cone (as shown in Figure 2(b)) was implemented, which gave better gas profiles albeit with some signs of perturbations. Lee and coworkers also found that the position and the direction of the pumping port were important in minimizing the sampling perturbation of the Laval expansion.

Here, a symmetric airfoil-shaped device has been designed as an alternative method for sampling the pulsed Laval expansion with minimal perturbation. This particular aerodynamic geometry favors the evacuation of thermalized gases as the gas pulse flows over the apex of the airfoil and allows photoionization of reactive gases as close as possible to the pinhole as indicated in Figure 2(a). Shown in Figure 3 is an orthographic projection with characteristic dimensions of the sampling device which is welded onto an 8" double-sided flange that is inserted between the source and detection chambers. The dimensions of the ellipse used to form the airfoil are as follows: a = 36 cm and b = 4.4 cm for the semi-major and semi-minor axis respectively. The ion extraction lens of the quadrupole mass spectrometer is located 20 mm below the apex of the airfoil, which ensures optimal collection efficiency of ions created in between the airfoil and the entrance of the quadrupole. The ions are then focused inside the quadrupole mass filter and are ultimately detected by a channeltron.

Figure 4 presents a comparison of sampled concentration profiles from the airfoil used in the present work and the skimmer implemented by Lee and coworkers (see caption). The ideal signal, which is the duration of the applied voltage to the pulsed valve, is shown for comparison. Clearly, there are marked improvements with the airfoil sampling technique. The onset of the ion signal observed with the airfoil is relatively sharp, followed by a plateau and drops to a minimum (see dotted lines in Figure 4(a) and (b), indicating the pre-pulse background signal level) when the pulsed valves are closed. The small rise and fall times in the ion signal are likely due to the inertia of the pulsed valves in reaching fully open or fully closed positions, i.e. the perturbation of the signal due to the airfoil is negligible. Note that no "tail" is observed with the airfoil after the arrival of the gas pulse as observed in the earlier skimmer sampling, shown in Figure 4(b). This indicates that the thermalized gases do not reflect back into the Laval expansion region and are effectively evacuated with this new sampling technique. Also, the pulsed beam profile measured with the quadrupole mass spectrometer is in excellent agreement with impact pressure measurements with a pressure transducer (not shown here).

2.3. Validity of kinetics measurements

Kinetic traces measured by time-resolved mass spectrometry are a convolution of the true kinetic behavior of the reactants and products as well as the finite instrument response function. Recently Taatjes[24] reinvestigated[25] the effects of the source velocity distribution on the determination of rate coefficients by time-resolved concentration measurements. Rules of thumb for designing valid experiments are derived for both effusive and supersonic beams. As described by Osborn and coworkers[20] in a paper on the design of the multiplexed photoionization mass spectrometer, the two dominant contributions to the instrument response in probing molecular concentrations are: (1) the distance separating the point of ionization from the pinhole and (2) the spread in molecular velocities. In effect, the time dependent molecular concentration sampled at a given point in time is both delayed by the velocity and by the spread in the velocity distribution of the molecular species of interest.

In the case of a collimated Laval beam, the expansion is supersonic. It follows that molecules move at the same velocity as the carrier gas in the beam. As a consequence, the propagation delay of the molecules from the pinhole to the point of ionization does not depend on mass, unlike an effusive source. Also, the velocity spread in the bulk gas flow is smaller. Taatjes[24] calculated the predicted response of sampling 13 cm from the skimmer opening used by Lee and coworkers. Based on the velocity in a supersonic expansion compared to an effusive beam, Taatjes concluded that the fidelity of the supersonic beam sampling is sufficient to probe fairly rapid decay transients, acknowledging the fact that calculating the detailed characteristics of a supersonic expansion is complex. Note that flow calculations based on molecular beam characteristics and geometry of the airfoil is outside the scope of this paper. For example, the density in the Laval expansion is sufficiently high for further cooling to occur after the pinhole, which will slightly improve the fidelity. In the conditions of Mach 3.35 Laval experiments, it was noted that pseudo first order exponential decays (hereafter noted as k_{obs}) approaching 25000 s^{-1} would be underestimated by less than 20 %.

In designing valid experiments to measure kinetics, it is useful to estimate the maximum exponential decays k_{obs} that can be measured as a function of the ionization distance x from the pinhole. Taatjes gives a rule of thumb for kinetic measurements that will be underestimated by less that 10 % in supersonic sampling. This approximate criterion can be expressed as follows:

$$\frac{\sqrt{\frac{2kT}{m}}\, x k_{obs}}{\left(\sqrt{\frac{2kT}{m}} + u\right)^2} < 0.1 \qquad (1)$$

where k is the Boltzman constant, T = 70 K is the source temperature, m = 28 under typical experimental conditions (N$_2$ as carrier gas) and u = 675 m/s is the bulk velocity (typical for a Mach 4 nozzle). Shown in Figure 5 is a plot of the maximum k_{obs} as a function of ionization distance with typical conditions observed for the Mach 4 nozzle. It is clear from this plot that x should be as small as possible to probe fairly rapid reactions. Typically 20000 < k_{obs} < 80000 s^{-1} as observed with our chemiluminescence

measurements. Therefore to measure first-order rate constants with good fidelity for k_{obs} < 80000 s^{-1}, the ionization point should be within 4 mm from the pinhole.

2.4. Detection chamber with quadrupole mass spectrometry

After being sampled, reactive gases from the Laval expansion are photoionized with VUV synchrotron radiation from the Advanced Light Source and mass analyzed. With a 450 µm pinhole in the airfoil that serves as a partition that allows for differential pumping, the pressure in the detection chamber is maintained at ~10^{-7} Torr using two 2000 L/s turbomolecular pumps when the pulsed valves are operating (10 Hz and 5 ms gas pulse duration). In this configuration experiments with a flow density of 10^{16} – 10^{17} molecules/cm^3 can be performed.

The goal of measuring rate coefficients for radical-neutral chemical reactions close to collision-determined limits led to the choice of ion detection via a quadrupole mass spectrometer (Hiden Analytical, Model IDP). Ions are probed continuously in a similar fashion to photon detection with a photomultiplier tube for chemiluminescence and LIF measurements. The 4-lens ion optics quadrupole filters (9 mm pole diameter), the secondary electron multiplier (SEM) detector and software were purchased from Hiden Analytical. The ion counting output of the SEM detector is fed into a 4-input multiple-event time digitizer (FAST COMTec P7886/P7888 model) for data collection. The overall diameter of the quadrupole analyzer is 17.4 mm, which is sufficiently small to be inserted as close as possible to the pinhole and ionization region in the airfoil sampling device. The apparatus is run at a 10 Hz repetition rate. Synchronization of the various experimental components is achieved using a digital delay generator (Stanford Research Systems, model DG535).

3. Results

The uniformity of the Laval expansions has been fully characterized by impact pressure and stagnation pressure measurement as described previously.[13] Typically, with the Mach 4 nozzle a uniform flow is obtained over 20 cm, which corresponds to 300 µs in time with v_{flow} = 675 m/s. As discussed in the previous section, the apparatus should be able to measure, with good fidelity, k_{obs} < 80000 s^{-1} for an ionization point 4 mm behind

the pinhole. Consider an initial concentration of transient species, $[C]_0$, involved in a pseudo-first order radical-neutral reaction with $k_{obs} = 80000$ s^{-1}. It can be assumed that the reaction is completed when the concentration of transient species drops to less that 1 % within 60 µs. Similarly, assuming 99 % completion for a chemical reaction in the available kinetic window of 300 µs, the lower limit for rate measurements is equal to 15000 s^{-1}.

As seen in Figure 4, the measured ion signal reaches a plateau within 500 µs of the initial rise, indicating that uniform flow conditions are achieved. Typically, the photolysis laser is pulsed with a 3 ms delay with respect to the opening of the pulsed valve, initiating the chemical reaction in the collimated flow. In the following two sections, we give a brief description of the capabilities of the apparatus in rate constant measurements and product identification using the model reaction of C$_2$H with acetylene, an important reaction for Titan's photochemistry.

3.1. Rate constant measurements

The reaction of C$_2$H with acetylene (Eq. 2) with the Mach 4 nozzle (70 K) was chosen as a test reaction to validate the kinetic and product detection measurements for the novel instrument described here.

$$C_2H + C_2H_2 \rightarrow C_4H_2 + H \qquad (2)$$
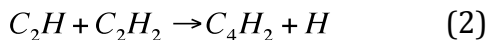
C$_2$H radicals are generated by pulsed laser photolysis of acetylene with an excimer laser at 193 nm. Since the measured percentage depletion of C$_2$H$_2$ is ~0.5 % at fluences typical of the excimer laser used here,[16] it can be assumed that the concentration of C$_2$H is much lower than the concentration of C$_2$H$_2$. Transient C$_2$H species are consumed in the radical-molecule reaction with the excess C$_2$H$_2$ producing stable C$_4$H$_2$ molecules after elimination of a H atom. The evolution of the intensity of the C$_4$H$_2^+$ signal (m/z = 50) under pseudo-first-order conditions can be expressed by Eq. 3.

$$\left[C_4H_2\right]_t = \left[C_2H\right]_0\left(1 - \exp(-k_{obs}t)\right) \qquad (3)$$

As demonstrated by Lee and coworkers, it is possible to measure the exponential rise of the product ion signal in order to extract the bimolecular rate coefficient of reaction,

$k = k_{obs}/[C_2H_2]_0$ at various concentrations of C_2H_2 under pseudo-first-order conditions. Shown in Figure 6 is a plot of the intensity of the $C_4H_2^+$ ion signal (in counts/s) at m/z = 50 as a function of reaction time obtained by accumulating ~20000 laser pulses. The plot can be divided into two portions, labeled A and B, which are described below.

After being focused into the quadrupole mass filters, ions propagate to the channeltron detector. The delay observed from the pulsing of the laser (t = 0) and the onset of the ion signal corresponds to the time-of-flight of the ions, t_0, which depends in part on the extractor voltage at the entrance of the QMS and the bias voltage applied to the quadrupole mass filters. For m/z = 50, $t_0 \approx 70$ μs with the optimized settings of the QMS. After this delay, the intensity of the ion signal rises and reaches a plateau. This behavior is characteristic of a fast forming reaction product, as would be expected of C_4H_2 in the reaction of C_2H with C_2H_2. The portion of the graph labeled A corresponds to the available kinetic window, i.e. the time interval corresponding to the sampling of the irradiated uniform column of gas extending from the pinhole to the exit of the Laval nozzle situated at 17 cm. This time interval also delimits the validity of a single exponential fit. The transient C_4H_2 signal, for 70 < t < 300 μs, can be fit by a single-exponential rise (shown as a black curve in Figure 6), yielding $k_{obs} = 22700 \pm 500$ s^{-1}, which indicates that the reaction is completed within 150 μs.

The time profile of the signal for t > 300 μs (i.e., right-hand portion labeled B) in Figure 6 is consistent with the sampling of the remaining irradiated gas that is inside the Laval nozzle and the reservoir block when the photolysis laser is pulsed. Indeed, in theory the pressure is a maximum in the flow at the throat of the nozzle and decreases inside the nozzle to reach a constant value in the collimated flow. The appearance of a maximum in the signal (portion labeled B) would correspond to stronger absorption of the excimer light at the throat of the nozzle because of a higher C_2H_2 density and consequently a higher C_4H_2 signal. However, the total absorption of the excimer light is small and thus the laser fluence is still uniform axially. Increasing the length of collimated gas, i.e. between 0.09 m and 0.18 m, by translation of the reservoir block along the axis of the beam with the linear shift causes this maximum in the ion signal to be delayed as observed in Figure 7. We have used this approach to measure the beam

velocity as another means of characterizing the uniformity of the Laval flow. This provides further evidence that the airfoil is not perturbing the collimated flow.

Plotting k_{obs} vs. $[C_2H_2]_0$ as shown in Figure 8 yields a rate coefficient of $(1.2\pm0.3)\times10^{-10}$ cm^3/molecule/s at 70 K. The rate coefficient is in very good agreement with previously reported kinetic data in the same temperature range by Chastaing and coworkers $(1.27\pm0.03\times10^{-10}$ at 63 K with He as buffer gas).[26]

3.2. Product identification

Reactions of nonresonance-stabilized carbon-centered radicals with unsaturated hydrocarbons are expected to proceed via an intermediate formed with almost no activation energy.[16] Subsequently, the short-lived adduct decomposes to give final products whose isomeric product branching is dependent on the energy available in the system. For the reaction of C_2H radicals with C_2H_2, the rate coefficient exhibits almost no temperature and pressure dependence and is close to the collision-determined limit as shown in the previous section.[26] This behavior indicates that back dissociation of the adduct is negligible. As shown experimentally and theoretically, the entrance channel of the reaction is the attack of the π-electrons of C_2H_2 by C_2H to form an intermediate that in turn decomposes to form diacetylene as the final product, consistent with an addition-elimination reaction. The H-abstraction channel is also thermodynamically feasible. Ceursters and co-workers[27] have calculated that the direct H-abstraction has a barrier of ~ 40 kJ/mol while the terminal addition is barrier-free. In such reactions involving the C_2H radicals with unsaturated hydrocarbons, addition-elimination should predominate over abstraction reactions. Therefore, an investigation into H-abstraction in the reaction of C_2H with C_2H_2 seems unlikely and is outside the scope of this paper. Such a study would require using fully deuterated acetylene (C_2D_2) and 3,3,3-trifluoropropyne (CF_3-C_2H) as the C_2H precursor. Here we focus on the diacetylene formation channel. Shown in Figure 9 is the measured photoionization spectrum (ion yield versus wavelength) of m/z = 50. The intensity of the ion signal as a function of the photon energy is retrieved from the raw data by integrating over the whole reaction timescale of 300 μs. Note that the intensity of the ion signal prior to the pulsing of the photolysis laser is averaged for

1 ms for background subtraction. The synchrotron generated photon current at each energy is measured using a SXUV-100 photodiode (International Radiation Detectors, Inc.) and used to normalize the raw ion signal. Diacetylene has an IE of 10.17 eV with a sharp onset followed by a second onset at ~ 10.4 eV that corresponds to the direct ionization to the $v' = 1$ vibrational level of the cation. Our photoionization efficiency curve is in very good agreement with the room temperature measurement recorded by Goulay and coworkers.[22] Note that the sharp feature at ~ 11.2 eV which may be due to an autoionizing Rydberg state is also observed.

4. Conclusion

In this paper, we present a pulsed Laval nozzle apparatus that couples tunable VUV synchrotron photoionization and quadrupole mass spectrometry to study kinetics and isomer-resolved product branching of gas phase radical-neutral molecule reactions at low temperatures. We have designed a symmetric airfoil-shaped device to sample the thermally equilibrated low temperature Laval expansion. The gas pulse profile measured with photoionization mass spectrometry shows negligible signs of perturbations compared with skimmer sampling implemented by Lee and coworkers.[13] Also, time-resolved signals of the gas pulse are in very good agreement with impact pressure measurements in the flow. The apparatus enables the study of chemical kinetics involving highly reactive radical species, such as C_2H, with condensable unsaturated hydrocarbons at low temperatures. When coupled to VUV synchrotron sources of radiation, pulsed Laval nozzles demonstrate considerable promise for the study of fast chemical kinetics at low-temperatures, especially in the field of planetary atmospheres.

References

(1)   Atkinson, D. B.; Smith, M. A. *Review of Scientific Instruments* **1995**, *66*, 4434.

(2)   Hansmann, B.; Abel, B. *Chemphyschem* **2007**, *8*, 343.

(3)   Niemann, H. B.; Atreya, S. K.; Demick, J. E.; Gautier, D.; Haberman, J. A.; Harpold, D. N.; Kasprzak, W. T.; Lunine, J. I.; Owen, T. C.; Raulin, F. *Journal of Geophysical Research-Planets* **2010**, *115*.

(4)   Waite, J. H.; Niemann, H.; Yelle, R. V.; Kasprzak, W. T.; Cravens, T. E.; Luhmann, J. G.; McNutt, R. L.; Ip, W. H.; Gell, D.; De La Haye, V.; Muller-Wordag, I.; Magee, B.; Borggren, N.; Ledvina, S.; Fletcher, G.; Walter, E.; Miller, R.; Scherer, S.; Thorpe, R.; Xu, J.; Block, B.; Arnett, K. *Science* **2005**, *308*, 982.

(5)   Krasnopolsky, V. A. *Icarus* **2009**, *201*, 226.

(6)   Hebrard, E.; Dobrijevic, M.; Pernot, P.; Carrasco, N.; Bergeat, A.; Hickson, K. M.; Canosa, A.; Le Picard, S. D.; Sims, I. R. *Journal of Physical Chemistry A* **2009**, *113*, 11227.

(7)   Lebonnois, S. *Planetary and Space Science* **2005**, *53*, 486.

(8)   Smith, I. W. M. *Chemical Society Reviews* **2008**, *37*, 812.

(9)   Rowe, B. R.; Dupeyrat, G.; Marquette, J. B.; Gaucherel, P. *Journal of Chemical Physics* **1984**, *80*, 4915.

(10)   Dupeyrat, G.; Marquette, J. B.; Rowe, B. R. *Physics of Fluids* **1985**, *28*, 1273.

(11)   Carty, D.; Le Page, V.; Sims, I. R.; Smith, I. W. M. *Chemical Physics Letters* **2001**, *344*, 310.

(12)   Vakhtin, A. B.; Heard, D. E.; Smith, I. W. M.; Leone, S. R. *Chemical Physics Letters* **2001**, *348*, 21.

(13)   Lee, S.; Hoobler, R. J.; Leone, S. R. *Review of Scientific Instruments* **2000**, *71*, 1816.

(14)   Taylor, S. E.; Goddard, A.; Blitz, M. A.; Cleary, P. A.; Heard, D. E. *Physical Chemistry Chemical Physics* **2008**, *10*, 422.

(15)   Goulay, F.; Rebrion-Rowe, C.; Biennier, L.; Le Picard, S. D.; Canosa, A.; Rowe, B. R. *Journal of Physical Chemistry A* **2006**, *110*, 3132.

(16)   Soorkia, S.; Trevitt, A. J.; Selby, T. M.; Osborn, D. L.; Taatjes, C. A.; Wilson, K. R.; Leone, S. R. *Journal of Physical Chemistry A* **2010**, *114*, 3340.

(17)   Goulay, F.; Leone, S. R. *Journal of Physical Chemistry A* **2006**, *110*, 1875.

(18)   Berteloite, C.; Le Picard, S. D.; Birza, P.; Gazeau, M. C.; Canosa, A.; Benilan, Y.; Sims, I. R. *Icarus* **2008**, *194*, 746.

(19)   Trevitt, A. J.; Goulay, F.; Taatjes, C. A.; Osborn, D. L.; Leone, S. R. *Journal of Physical Chemistry A* **2010**, *114*, 1749.

(20)   Osborn, D. L.; Zou, P.; Johnsen, H.; Hayden, C. C.; Taatjes, C. A.; Knyazev, V. D.; North, S. W.; Peterka, D. S.; Ahmed, M.; Leone, S. R. *Review of Scientific Instruments* **2008**, *79*.

(21)   Soorkia, S.; Taatjes, C. A.; Osborn, D. L.; Selby, T. M.; Trevitt, A. J.; Wilson, K. R.; Leone, S. R. *Physical Chemistry Chemical Physics* **2010**, *12*, 8750.

(22)   Goulay, F.; Osborn, D. L.; Taatjes, C. A.; Zou, P.; Meloni, G.; Leone, S. R. *Physical Chemistry Chemical Physics* **2007**, *9*, 4291.

(23)   Sabbah, H.; Biennier, L.; Klippenstein, S. J.; Sims, I. R.; Rowe, B. R. *Journal of Physical Chemistry Letters* **2010**, *1*, 2962.

(24)   Taatjes, C. A. *International Journal of Chemical Kinetics* **2007**, *39*, 565.

(25)   Moore, S. B.; Carr, R. W. *International Journal of Mass Spectrometry and Ion Processes* **1977**, *24*, 161.

(26)   Chastaing, D.; James, P. L.; Sims, I. R.; Smith, I. W. M. *Faraday Discussions* **1998**, *109*, 165.

(27)   Ceursters, P.; Nguyen, H. M. T.; Peeters, J.; Nguyen, M. T. *Chemical Physics* **2000**, *262*, 243.

Captions for Figures

Figure 1: Section view of the pulsed Laval nozzle apparatus with quadrupole mass spectrometry and airfoil sampling geometry.

Figure 2: Comparison between (a) airfoil sampling in this work and (b) skimmer sampling implemented by Lee and coworkers. The pump-out ports in the source and detection regions are indicated: TP for turbomolecular pump, MP for mechanical pump and DP for diffusion pump.

Figure 3: Orthographic view of the airfoil used for sampling in the apparatus described here. All dimensions are in inches.

Figure 4: Comparison of pulsed gas profiles obtained with airfoil and skimmer sampling. (a) C_4H_6 ion signal (1 % 1,3-butadiene in N_2 carrier gas) obtained by VUV synchrotron photoionization (10.6 eV) at a distance < 1 mm after the pinhole of the airfoil. (b) Pulsed gas profile obtained with laser photoionization at a distance of 130 mm with 30° entrance angle, 6 cm long skimmer by Lee and coworkers.[13] The ideal signals (black square pulse) are also indicated, which correspond to the duration of the voltage applied to the pulsed valves, i.e. 6.5 ms in this work and 5 ms by Lee and coworkers. It is clear that no "tail" is observed in the gas profile in (a) as opposed to (b). This residual effect is attributed to perturbation in the Laval expansion by thermalized gases that accumulate around the skimmer. No such effect is observed with the symmetric airfoil sampling device.

Figure 5: Predicted maximum $k_{obs}(s^{-1})$ that will be underestimated by less than 10 % plotted as a function of the ionization point from the pinhole x (mm). The values are computed using Eq. 1 (see text) with $T = 70$ K and $u = 675$ m/s, which are typically observed with the M4 nozzle.

Figure 6: Time-resolved ion signal of m/z = 50 ($C_4H_2^+$) in the reaction of ethynyl radicals with acetylene. See text for explanation.

Figure 7: Beam velocity determination using the position of the maximum of photolysis product produced at the throat of the nozzle (see text). (a) Methyl radical transit time as a

function of the distance between the exit of the Laval nozzle and the pinhole. (b) Distance from pinhole versus arrival time of methyl radicals formed at the throat, the slope of which yields the beam velocity. Error bars are given as ± 0.01 ms for arrival times and ± 0.005 m for distances.

Figure 8: Plot of k_{obs} from exponential fits of C_4H_2 concentration profiles as a function of acetylene concentration.

Figure 9: Photoionization spectrum of m/z = 50 from the reaction of C_2H with C_2H_2 (open circles). The black curve is a diacetylene PIE curve recorded by Goulay and coworkers.[22]

List of figures

TMP (2000 L/s)

Source chamber   VUV light

Detection chamber

Linear shift

QMS

Laser beam

Laval nozzle

Airfoil

Roots blower (1200 m³/h)

TMP (2000 L/s)
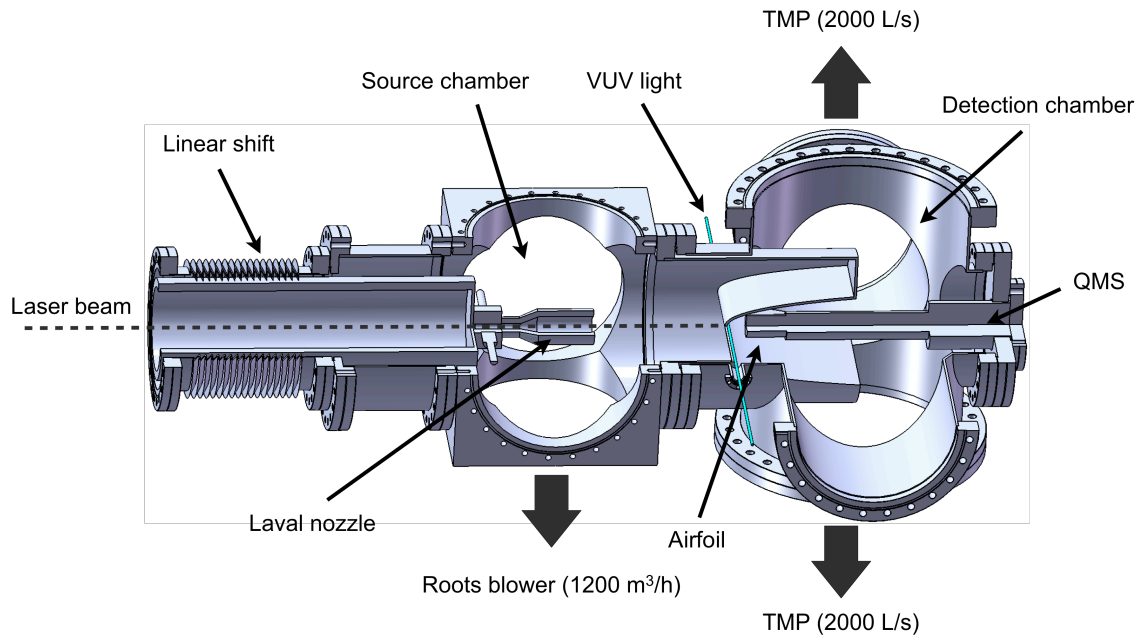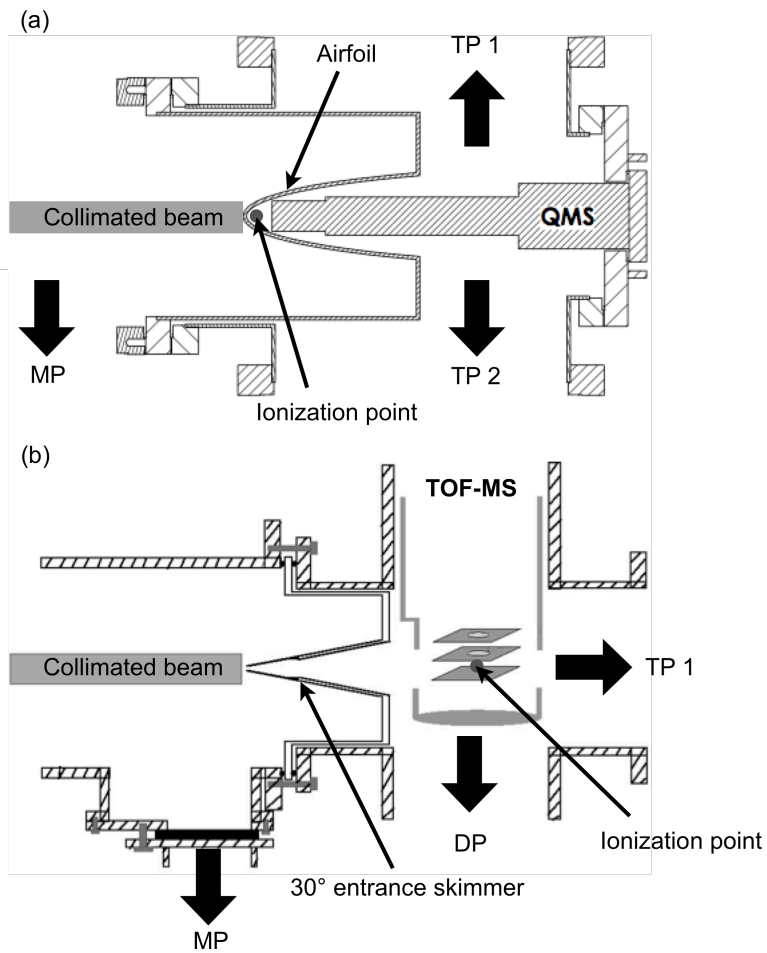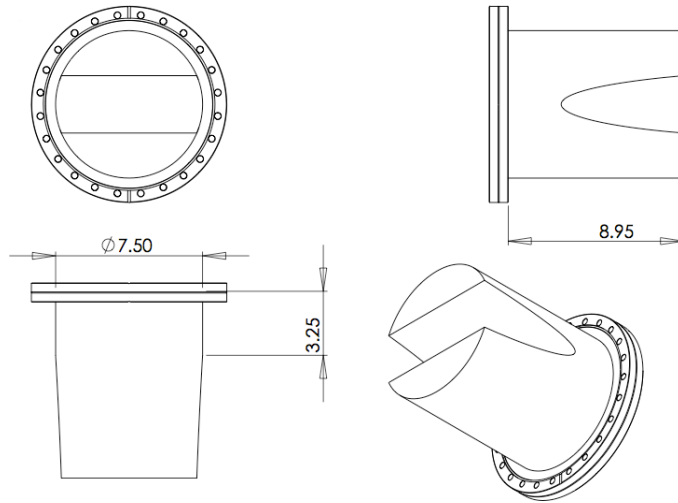
Figure 1

Figure 2

Figure 3
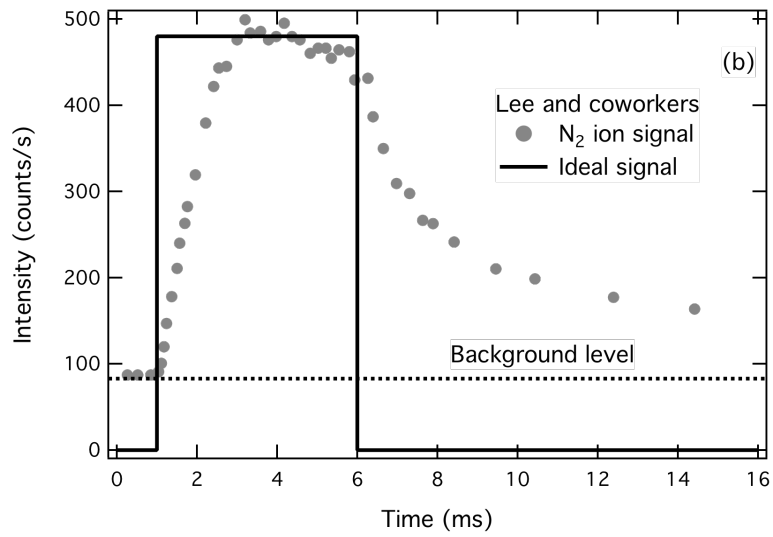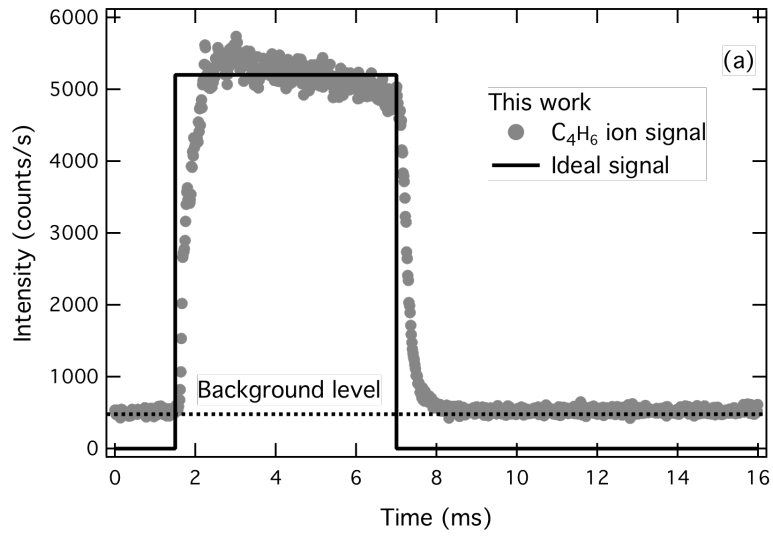
Figure 4
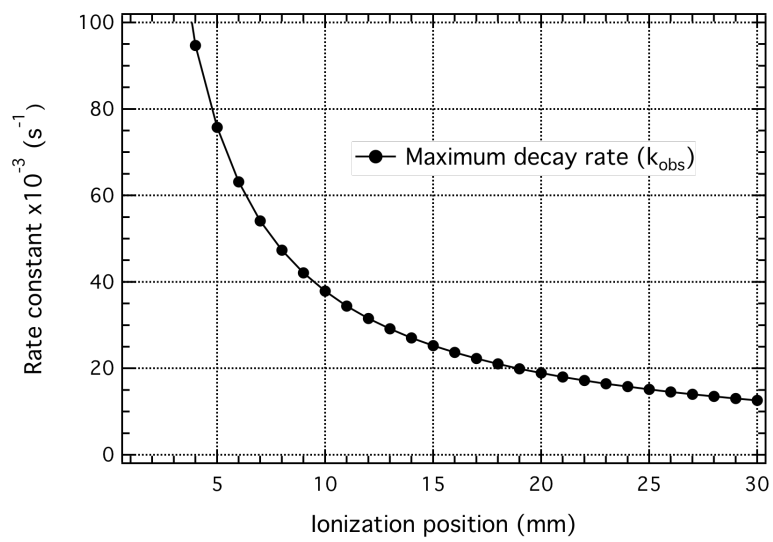
Figure 5
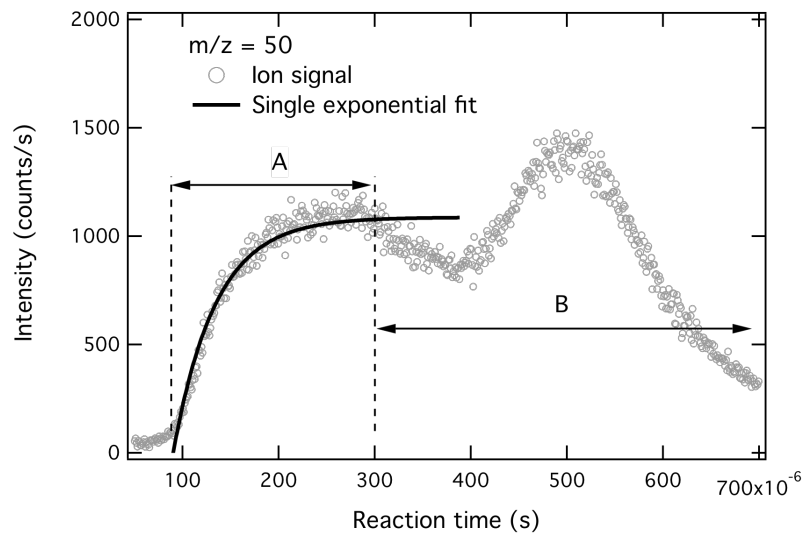
Figure 6

Figure 7

Figure 8

Figure 9